AT&T BELL LABORATORIES TECHNICAL JOURNAL
Vol. 63, No. 3, March 1984
Printed in U.S.A.

Performance of Cross-Polarized M-ary QAM Signals Over Nondispersive Fading Channels

By M. KAVEHRAD*

(Manuscript received June 1, 1983)

This paper presents performance analysis of dual-polarized M-ary Quadrature Amplitude Modulated (QAM) signals over nondispersive radio channels. In particular, dual-polarized, 16-QAM signals are examined. A simple method for adaptive cancellation of static and fade-induced cross-polarization interference is introduced. The cancellation is performed at baseband. For this canceler, two adaptation methods are studied. The results indicate that dual-polarized M-ary QAM is not feasible over fading channels unless means of adaptive cancellation of the cross-polarization interference are provided. The results also indicate that the adaptive algorithm employed in cross-polarization interference cancellation should take into account noise power reduction.

I. INTRODUCTION

Consider transmission of two orthogonally polarized Quadrative Amplitude Modulated (QAM) carriers over a single communication route. As an example, envision a dual-polarization radio communication system where the available bandwidth is "reused" in order to double the route capacity by transmitting two independent M-ary QAM signals over the same Radio Frequency (RF) channel, using orthogonally polarized waves. Because of channel impairments, such as fades or antenna imperfections, however, the orthogonally polarized waves are received depolarized at the receiver. Consequently, there

* AT&T Bell Laboratories.

will be some interference imposed on each signal, causing errors in the detection process. We refer to this effect as cross-polarization (x-pol) distortion. For such a case, the x-pol parameters have randomly time-variant characteristics unknown to the receiver in advance.

Several methods for canceling the x-pol distortion (XPD) in dual-polarized systems have been proposed by investigators.[1-5] The first two references assume access to some beacon signals for cancellation of the x-pol distortion. For instance, Chu[2] considers the use of two pilot tones, one for each polarization, to estimate the scattering matrix of the radio channel, and applies a differential phase and attenuation in the receive antenna feed to eliminate the x-pol interference and restore the orthogonality. Steinberger[3] proposes a recursive equalization structure that operates at RF and experimentally shows that the device can cancel the x-pol distortion induced by fades over a terrestrial radio link when dual-polarized eight-phase shift keying signals are employed. RF/IF x-pol cancellation schemes are suitable when the dual-polarized signals have to be transmitted over several nonregenerative hops, with cancellation occurring on each hop. Such might be the case in many terrestrial radio communication applications where, by avoiding baseband x-pol cancellation, the operation is more cost-effective in terms of a reduced number of required modems. However, for digitally modulated carriers, especially if used over a regenerative transmission hop, the x-pol distortion can be eliminated directly at baseband as a part of the information detection process. Attempts in the area of baseband x-pol cancellation have been made by Culmone,[4] and Nichols et al.[5]

In this study we suggest a very simple adaptive baseband canceler to eliminate the x-pol distortion in dual-polarized M-ary QAM systems. Two methods of canceler taps adaptation are evaluated. We analyze the performance of such systems by deriving an average probability of error as a function of signal-to-noise ratio (s/n), x-pol distortion, and nondispersive fade level with or without the baseband canceler. The results indicate that over a typical fading radio channel with static x-pol of about -25 dB, dual polarization of M-ary QAM signals is possible only if some x-pol distortion cancellation method is employed. In Section II, we explain the mathematical modeling of the dual channel. The adaptive baseband canceler is described in Section III. Section IV presents the performance analysis of dual-polarized, M-ary QAM systems with or without x-pol distortion cancellation. Section V gives the numerical performance results for 16-QAM systems. It should be noted that even though the analysis is a baseband analysis, the results are also applicable to RF or Intermediate Frequency (IF) cancellation systems employing similar adaptation algorithms.

II. DUAL-POLARIZATION CHANNEL MODEL

We consider transmission of two independent, orthogonally M-ary QAM carriers with the same bandwidth and center frequency. The bandpass signal on either of the two orthogonal channels can be represented by

$$S_i(t) = R_e\{\tilde{s}_i(t)\exp(j\omega_c t)\}, \qquad i = 1, 2, \tag{1}$$

where $R_e\{\cdot\}$ denotes the real part, $\tilde{s}_i(t)$ is the low-pass complex envelope, and ω_c is the nominal carrier frequency. The complex envelope can be expressed as

$$\tilde{s}_i(t) = \sum_{m=0}^{\infty} \tilde{\alpha}_i(m)\tilde{h}(t - mT), \qquad i = 1, 2, \tag{2}$$

where $\tilde{\alpha}_i(m)$ denotes the complex-valued information symbol stream, and $\tilde{h}(t)$ is the complex low-pass equivalent of the overall system impulse response. The complex-valued symbols are denoted by

$$\tilde{\alpha}_i(m) = \delta_i(m) + j\beta_i(m), \qquad i = 1, 2,$$

where $\delta_i(m)$ and $\beta_i(m)$ take on elements of the set $\{\pm c, \pm 3c, \cdots, \pm(L-1)c\}$, with $L = \sqrt{M}$, and M the number of levels of the M-ary signal. The parameter, L, is chosen to be even. The constant, c, denotes the distance of each point in the signal constellation from its nearest decision region boundary. The random variables, $\delta_i(m)$ and $\beta_i(m)$, are identically distributed and take on the specified values with equal probability. Note that in eq. (1) it is assumed that the data sequences are synchronized and carrier signals are coherent. These assumptions, however, may not be necessary in practice.

The channel is assumed to be of the slowly time-variant nondispersive type that takes two independent streams of data and distorts the transmission by introducing a fraction of one stream into the other. A practical model of such a channel might be a satellite channel with rain-induced attenuation and depolarization, which is usually nondispersive across the channel bandwidth; hence, depolarization of the dual-polarized signals over such a channel resembles the described scenario.

It is known that deep multipath fading of the main polarization signals on microwave radio routes, in general, is dispersive. However, because of the lack of empirical data concerning the dispersiveness of the cross-polarized parameters, we confine this analysis to those radio channels where all the signals are subjected to nondispersive fading (for example, satellite channels).

The dual channel matrix is characterized by

$$\mathbf{A} = \begin{bmatrix} a_{11} & a_{12} \\ a_{21} & a_{22} \end{bmatrix}, \tag{3}$$

in which the a_{jk}'s, $j = 1, 2$, $k = 1, 2$, are complex-valued quantities used to represent the channel attenuation and phase shift. These quantities are randomly time variant; however, the time variations are assumed to be slow in comparison to the symbol rate of the signals. Such slow variations can be tracked and canceled adaptively. The received low-pass equivalent signals can be expressed as

$$\begin{cases} r_1(t) = a_{11}\tilde{s}_1(t) + a_{12}\tilde{s}_2(t) + \eta_1(t) \\ r_2(t) = a_{21}\tilde{s}_1(t) + a_{22}\tilde{s}_2(t) + \eta_2(t), \end{cases} \tag{4}$$

where $\eta_1(t)$ and $\eta_2(t)$ are independent, zero-mean, white Gaussian processes. The received signals are filtered by receive filters matched to the transmit signals and sampled at every symbol period. The sampled signals are denoted by $x_i(k)$, $i = 1, 2$, and are expressed as

$$\begin{cases} x_1(k) = a_{11}\tilde{\alpha}_1(k) + a_{12}\tilde{\alpha}_2(k) + n_1(k) \\ x_2(k) = a_{21}\tilde{\alpha}_1(k) + a_{22}\tilde{\alpha}_2(k) + n_2(k). \end{cases} \tag{5}$$

The colored noise sequences, $\{n_1(k)\}$ and $\{n_2(k)\}$, are independent samples of zero-mean, complex-valued Gaussian processes with equal variances

$$E\{|\, n_i(k)\,|^2\} = \sigma_n^2, \qquad i = 1, 2,$$

where $E\{\cdot\}$ denotes the statistical average. The factors a_{11} and a_{22} represent the in-line attenuation and phase shift; the factors a_{12} and a_{21} represent the x-pol coupling on the two channels.

Data calculated by Chu[6] show that for linearly polarized waves, the behavior of the cross-polarized signal amplitude can be described by

$$\overline{\text{XPL}} = \frac{|\, a_{ij}\,|^2}{|\, a_{ii}\,|^2}, \qquad i = 1, 2, \qquad j = 1, 2, \qquad i \neq j, \tag{6}$$

where $\overline{\text{XPL}}$ is defined as cross-polarization factor of linearly polarized waves[6] and

$$\overline{\text{XPL}} = \frac{1}{2}\left(\frac{C}{D}\, e^{-4\sigma_\Theta^2}\right)[1 - \cos(4\tau e^{-8\sigma_m^2})]\delta, \tag{7}$$

where σ_m is the standard deviation of time-varying, mean-canting angle Θ_m over various rainstorms, σ_Θ is the standard deviation of anistropy angle Θ, τ is the orientation angle of the quasi-vertical

polarization, δ is proportional to in-line attenuation factor, and C/D is proportional to differential propagation constants. Measured data from COMSTAR II follow these calculations closely.[6] The comparison is shown in Fig. 1 of Ref. 6. We will use these results to introduce an average probability of error as a function of in-line attenuation level.

In the next section we describe a simple structure that can reduce the x-pol distortion in such systems.

III. ADAPTIVE BASEBAND CANCELER MODEL

The adaptive canceler that attempts to remove the x-pol distortion is characterized by

$$\mathbf{W} = \begin{bmatrix} w_{11} & w_{12} \\ w_{21} & w_{22} \end{bmatrix},$$

where w_{ij}'s, $i = 1, 2, j = 1, 2$ are the canceler coefficients. This adaptive device, which is a part of the M-ary QAM detector circuit, is studied under two adaptation methods. The first method employs a Least Mean-Square (LMS) error algorithm and the second applies channel matrix diagonalization. Figure 1 shows the LMS canceler structure. The samples at the matched filter output of each receiver are inputs to a bank of adaptive filters formed by a set of multiplier accumulators (MACs). To update the coefficients of the canceler, each MAC contains storage elements for storing the result of the multiplication of the signal-sample detection error and the complex conjugate of the corresponding received signal sample at the matched filter output. The calculated coefficients are multiplied by the signal samples at the matched filter output and used to cancel the x-pol distortion. The detectors shown in Fig. 1 are part of the M-ary QAM demodulators.

The canceler structure consists of a simple adaptive filter, which minimizes the least mean-square error in symbol estimation. The theory of this type of filter is well known[7] and is solely based on the statistical orthogonality principle. According to this theory, mean-square error is minimum when the error in symbol estimation is statistically orthogonal to the variable being observed. In the case at hand, we show the signal-sample estimation error by

$$\epsilon_i(k) = \hat{\alpha}_i(k) - \tilde{\alpha}_i(k), \qquad i = 1, 2, \tag{8}$$

where $\hat{\alpha}_i(k)$ is the detector input, as shown in Fig. 1. We now select those canceler coefficients for which the mean-square error is minimum, i.e., the results of solving min $E\{|\epsilon_1(k)|^2 + |\epsilon_2(k)|^2\}$. After proceeding with the minimization process, the following set of equations will lead to the optimum determination of the coefficients w_{ij}^0, $i = 1, 2, j = 1, 2$:

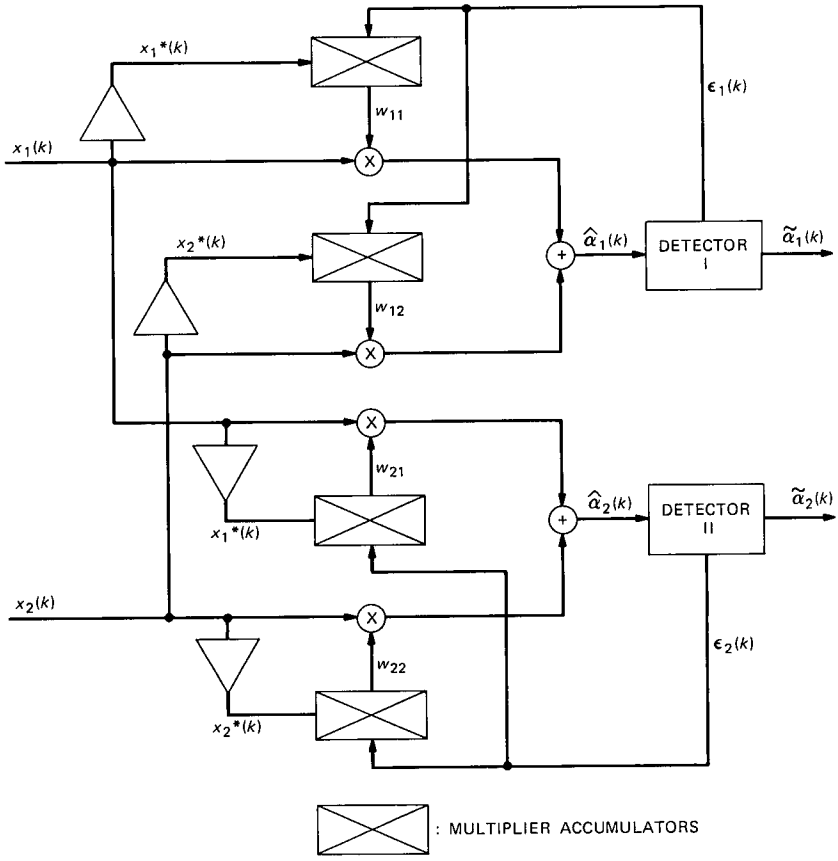

Fig. 1—Block diagram of adaptive LMS baseband canceler.

$$
\begin{aligned}
[|a_{11}|^2 + |a_{12}|^2 + \sigma_n^2]w_{11}^0 + [a_{21}a_{11}^* + a_{12}^*a_{22}]w_{12}^0 &= a_{11}^* \\
[a_{21}^*a_{11} + a_{12}a_{22}^*]w_{11}^0 + [|a_{21}|^2 + |a_{22}|^2 + \sigma_n^2]w_{12}^0 &= a_{21}^* \\
[|a_{11}|^2 + |a_{12}|^2 + \sigma_n^2]w_{21}^0 + [a_{21}a_{11}^* + a_{12}^*a_{22}]w_{22}^0 &= a_{12}^* \\
[a_{21}^*a_{11} + a_{12}a_{22}^*]w_{21}^0 + [|a_{21}|^2 + |a_{22}|^2 + \sigma_n^2]w_{22}^0 &= a_{22}^*. \qquad (9)
\end{aligned}
$$

As Fig. 1 shows, the signal samples at the canceler output for each channel can be expressed as

$$
\begin{cases}
\hat{\alpha}_1(k) = w_{11}x_1(k) + w_{12}x_2(k) \\
\hat{\alpha}_2(k) = w_{21}x_1(k) + w_{22}x_2(k),
\end{cases} \qquad (10)
$$

where $\hat{\alpha}_1$ and $\hat{\alpha}_2$ are complex quantities. In eq. (10), by substituting $x_m(k)$'s, $m = 1, 2$ of eq. (5) and the coefficients w_{ij}^0, $i = 1, 2, j = 1, 2$ of

eq. (9), one can form a decision variable for each channel for the derivation of probability of error.

An alternate solution to this type of optimization problem, which uses the steepest descent algorithm and is simple to implement, was suggested by Widrow.[8] The solution is recursive and states that

$$w_{ij}^{(k+1)} = w_{ij}^{(k)} + \epsilon_i(k)x_j^*(k), \qquad i = 1, 2, \qquad j = 1, 2, \qquad (11)$$

where * denotes the complex conjugate and k represents the sampling instant. In eq. (11) the noisy estimates of the cross-correlation of the observed signal and error signal are used as unbiased estimates to update the canceler coefficients at every baud interval. Such algorithms are well known in adaptive filtering and equalization. The realization of eq. (11) is shown in Fig. 1. The MACs in the figure update eq. (11) by storing the result of multiplication of signal samples and detection error samples.

As an alternative adaptation method, we consider a case where the canceler coefficients are determined by forcing the x-pol interference on each channel to zero.[9] This is equivalent to diagonalizing the overall channel matrix; i.e., substituting $x_m(k)$'s of eq. (5) into eq. (10) and forcing the coefficient of the undesired signal to zero on each channel, i.e., by

$$\begin{cases} w_{11}a_{12} + w_{12}a_{22} = 0 \\ w_{21}a_{11} + w_{22}a_{21} = 0. \end{cases} \qquad (12)$$

In this case we refer to the canceler as a diagonalizer. Amitay describes the realization of an IF diagonalizer.[9] In analogy to intersymbol-interference removal by zero-forcing equalization, this method can also be referred to as zero-forcing cancellation. Figure 2 shows a block diagram of the diagonalizer. Note that in canceling the interference, the diagonalizer neglects the thermal noise completely.

In the following section we will evaluate the canceler for both cases described.

IV. SYSTEM PERFORMANCE ANALYSIS

In this section we derive an upper bound on the average probability of error for dual-polarized M-ary QAM signals with and without the x-pol distortion canceler. Throughout this section it is assumed the data sequences on the two polarized channels are independent, equally likely, M-ary QAM signals. The channel is characterized by the matrix introduced earlier. To simplify the derivation, with no loss of generality, we can assume the phase angles of a_{11} and a_{22} are zero and use the normalized notations

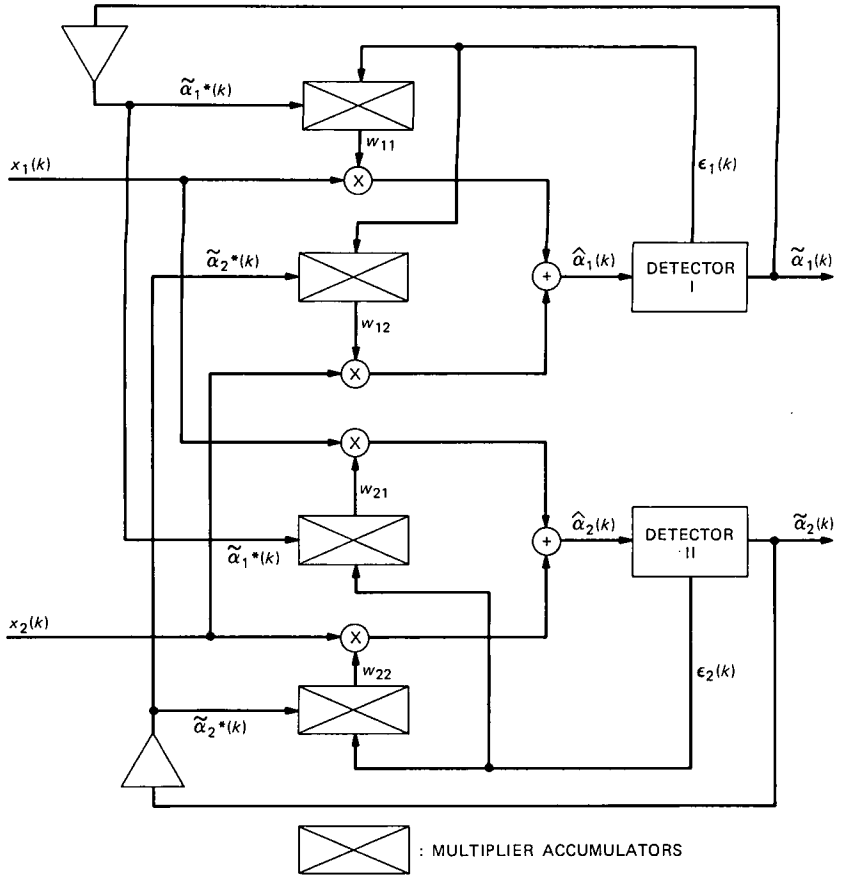

Fig. 2—Block diagram of adaptive diagonalizer.

$$\frac{a_{12}}{a_{11}} = \xi_1 \exp(j\phi_1),$$

$$\frac{a_{21}}{a_{22}} = \xi_2 \exp(j\phi_2),$$

and

$$\left| \frac{a_{11}}{a_{22}} \right| = \xi_o. \tag{13}$$

All the variables introduced in eq. (13) are time variant, but the time variations are slow relative to symbol rate so the receiver can obtain perfect estimates of the channel matrix components. The phase parameters ϕ_1 and ϕ_2 in eq. (13) are uniformly distributed over $[-\pi, \pi]$.

Also, to further simplify the presentation of the results, we assume $\xi_1 = \xi_2 = \xi$, and $\xi_0 = 1$. This model was shown by Chu to be a valid model for depolarization of dual-polarized waves due to heavy rainfall.[10] Furthermore, this simplified model of a x-pol channel still provides means of evaluating the canceler performance, and the error probability bounds derived should be useful in preliminary system planning.

4.1 Performance in the presence of the canceler

In this section we first derive an average probability of error applying the diagonalizer. Then we proceed with deriving an average error probability for the LMS canceler.

To calculate a simple upper bound on the probability of error performance when the diagonalizer is present, we use the complex valued estimates of the data symbols at the canceler output given in eq. (10), along with the constraints in eq. (12) and matched filter outputs of eq. (5), to define the following simplified decision variables for the two channels:

$$\begin{cases} \hat{a}_1(k) = a_{11}[1 - \xi^2 e^{j(\phi_1+\phi_2)}]\tilde{\alpha}_1(k) + n_1(k) - n_2(k)\xi e^{j\phi_1} \\ \hat{\alpha}_2(k) = a_{22}[1 - \xi^2 e^{j(\phi_1+\phi_2)}]\tilde{\alpha}_2(k) + n_2(k) - n_1(k)\xi e^{j\phi_2}. \end{cases} \tag{14}$$

As this equation shows, the decision variable for channel i depends on the parameters of channel j, $i \neq j$, $i = 1, 2, j = 1, 2$, namely, ϕ_j and n_j. Now consider the in-phase and quadrature-phase components of each channel. The decision variable for channel 1 in eq. (14) can be expressed in terms of its real and imaginary parts as

$$\begin{aligned} z_R(k) &= -\delta(k)\xi^2\cos(\phi_1 + \phi_2) + \beta(k)\xi^2\sin(\phi_1 + \phi_2) \\ &\quad + \frac{1}{a_{11}} n_{1R}(k) + \frac{1}{a_{11}} n_{2I}(k)\xi \sin(\phi_1) \\ &\quad - \frac{1}{a_{11}} n_{2R}(k)\xi \cos(\phi_1) \\ z_I(k) &= -\beta(k)\xi^2\cos(\phi_1 + \phi_2) - \delta(k)\xi^2\sin(\phi_1 + \phi_2) \\ &\quad + \frac{1}{a_{11}} n_{1I}(k) - \frac{1}{a_{11}} n_{2I}(k)\xi \cos(\phi_2) \\ &\quad - \frac{1}{a_{11}} n_{2R}(k)\xi \sin(\phi_2), \end{aligned} \tag{15}$$

where $n_{iR}(k)$ and $n_{iI}(k)$, $i = 1, 2$, are the real and imaginary parts of Gaussian noise samples at sampling instant k, which are identically distributed random variables with the same variance, σ_n^2. Now, an

error is made on channel 1 if $|z_R| > c$ or $|z_I| > c$, where c, as stated earlier, is the signal distance from its nearest decision region boundary in the signal constellation. Therefore, the probability of error on channel 1 can be expressed as

$$P_e = \frac{L-1}{2L}\{P_r(|z_R| > c) + P_r(|z_I| > c)\}. \tag{16}$$

To derive the error probability, we apply the well-known[11] Chernoff bound, which states

$$P_r\{z > c\} \leqslant \exp(-\lambda c)E\{\exp(\lambda z)\}, \qquad \lambda \geqslant 0, \tag{17}$$

where $E\{\cdot\}$ denotes the statistical average of the random variable z. This is valid for any $\lambda \geqslant 0$. Using the positive λ that minimizes the right-hand side of eq. (17) establishes the least upper bound. Hence, we apply eq. (17) to eqs. (15) and (16) combined. The actual derivation of the upper bound is in Appendix A.

The resulting probability of error bound is

$$P_e \leqslant \frac{L-1}{L}\exp\left[-\frac{3}{2(L^2-1)}\frac{\gamma|a_{ii}|^2}{1+\gamma\xi^4|a_{ii}|^2+\xi^2}\right], \qquad i = 1, 2, \tag{18}$$

where

$$\gamma = \frac{L^2-1}{3}\frac{c^2}{\sigma_n^2} = \text{the unfaded s/n}$$

$$|a_{ii}| = \text{the in-line voltage on channel } i, \qquad i = 1, 2.$$

We define

$$\text{XPD} = 20\log_{10}\xi, \text{ dB} \tag{19}$$

as a measure of x-pol distortion to represent the cross-coupling between the two channels, and

$$v = 20\log_{10}|a_{ii}|, \text{ dB} \qquad i = 1, 2 \tag{20}$$

as a measure of flat-fade level. When there is no fade, $v = 0$ dB and the only contribution to x-pol distortion is due to the static effects, such as antenna imperfections, in which case XPD is denoted by XPD_0. The fade-induced part of the x-pol distortion is put into effect when $|a_{ii}| < 1$, $i = 1, 2$. Now, eq. (7) can be applied to relate the average probability of error to in-line attenuation and to remove the x-pol factor in eq. (18). That is,

$$P_e(|a_{ii}|^2) \leq \frac{L-1}{L} \exp\left[-\frac{3}{2(L^2-1)} \cdot \frac{\gamma|a_{ii}|^2}{1+\gamma\,\overline{\mathrm{XPL}^2}|a_{ii}|^2+\overline{\mathrm{XPL}}}\right], \quad i=1,2. \tag{21}$$

We now proceed with reevaluating the probability of error when the LMS canceler is employed. As we stated in Section III, the LMS canceler adaptively calculates its coefficients so that the mean-square error is minimized. By using the optimum set of coefficients of eq. (9) in eq. (10), we can define a new decision variable for each channel; that is,

$$\begin{cases} \hat{\alpha}_1 = (w_{11}^0 a_{11} + w_{12}^0 a_{21})\tilde{\alpha}_1 + (w_{11}^0 a_{12} + w_{12}^0 a_{22})\tilde{\alpha}_2 \\ \qquad + w_{11}^0 n_1 + w_{12}^0 n_2 \\ \hat{\alpha}_2 = (w_{21}^0 a_{11} + w_{22}^0 a_{21})\tilde{\alpha}_1 + (w_{21}^0 a_{12} + w_{22}^0 a_{22})\tilde{\alpha}_2 \\ \qquad + w_{21}^0 n_1 + w_{22}^0 n_2, \end{cases} \tag{22}$$

where w_{ij}^0's are the optimum coefficients. As we see again, the decision variable for channel i depends on the parameters of channel j, $i \neq j$, $i = 1, 2, j = 1, 2$. In a manner similar to what was explained for the diagonalizer, we can calculate the probability of error for the LMS canceler. The actual derivation of the bound is in Appendix B. The resulting probability of error is

$$P_e \leq \frac{L-1}{L\pi} \int_0^{2\pi} \left(1-\frac{\phi}{2\pi}\right) \exp\left\{-\frac{3}{2(L^2-1)} \cdot \frac{\gamma\nabla(\phi)}{\gamma\Theta(\phi)+\Delta(\phi)}\right\} d\phi, \tag{23}$$

where

$$\gamma = \frac{L^2-1}{3}\frac{c^2}{\sigma_n^2},$$

and $\nabla(\phi)$, $\Theta(\phi)$, and $\Delta(\phi)$ are defined in eq. (34) of Appendix B. An attempt to solve eq. (23) in a closed form turned out to be inconclusive, so it was calculated on a computer numerically. To express eq. (23) only in terms of fade level, again we can use eq. (7) to remove ξ.

To make a comparison, we remove the canceler and repeat the derivation of the probability of error for a baseline, dual-polarized, M-ary QAM system.

4.2 Performance of baseline, dual-polarized, M-ary QAM system

In this case the error-bound derivation is simplified because for channel i the decision variables are independent of the other channel's

parameters, namely, ϕ_j and n_j, $j \neq i$, $i = 1, 2$, $j = 1, 2$. Therefore, eq. (15) is reduced to

$$\begin{cases} z_R(k) = \xi\delta_2(k)\cos(\phi_1) - \xi\beta_2(k)\sin(\phi_1) + \dfrac{1}{a_{11}} n_{1R}(k) \\ z_I(k) = \xi\beta_2(k)\cos(\phi_1) + \xi\delta_2(k)\sin(\phi_1) + \dfrac{1}{a_{11}} n_{1I}(k). \end{cases} \tag{24}$$

Using a similar approach, as for the previous cases, we derive an upper bound on the error probability. This derivation is given in Appendix C. The result is

$$P_e \leq \frac{L-1}{L} \exp\left\{-\frac{3}{2(L^2-1)} \frac{\gamma|a_{ii}|^2}{1+\gamma\xi^2|a_{ii}|^2}\right\}, \qquad i = 1, 2. \tag{25}$$

This is a simple bound to calculate, and in terms of fade level, it can be expressed as

$$P_e(|a_{ii}|^2) \leq \frac{L-1}{L} \exp\left[-\frac{3}{2(L^2-1)} \cdot \frac{\gamma|a_{ii}|^2}{1+\gamma|a_{ii}|^2 \cdot \overline{\text{XPL}}}\right], \qquad i = 1, 2. \tag{26}$$

The numerical results in the following section illustrate the performance.

V. NUMERICAL PERFORMANCE FOR 16 QAM

In this section we evaluate the bounds derived in the previous section for dual-polarized 16-QAM signals.

First, we consider 16 QAM with no cancellation. The upper bound of eq. (25) is shown in Fig. 3 for three different static x-pol distortion (XPD_0) values. These curves represent the average error probability bound for 16-QAM signals as a function of static x-pol distortion and s/n when no cancellation is adopted and no fading exists. Figure 3 also shows the theoretical performance of the 16 QAM and the theoretical calculated upper bound, i.e., for the case when there is no fade and no x-pol distortion. As we see, the upper bound curve is very close to the actual theoretical curve. These results indicate that improving the static x-pol can improve the overall performance substantially. Figure 4 demonstrates the bound in eq. (26) for 5-dB flat fade, using Fig. 1 of Reference 6, which predicts an $\overline{\text{XPL}}$ of 28 dB for a 5-dB flat fade. As we see, the sensitivity of the error probability to the fade level is quite high.

Next, we apply the canceler and the diagonalizer described earlier

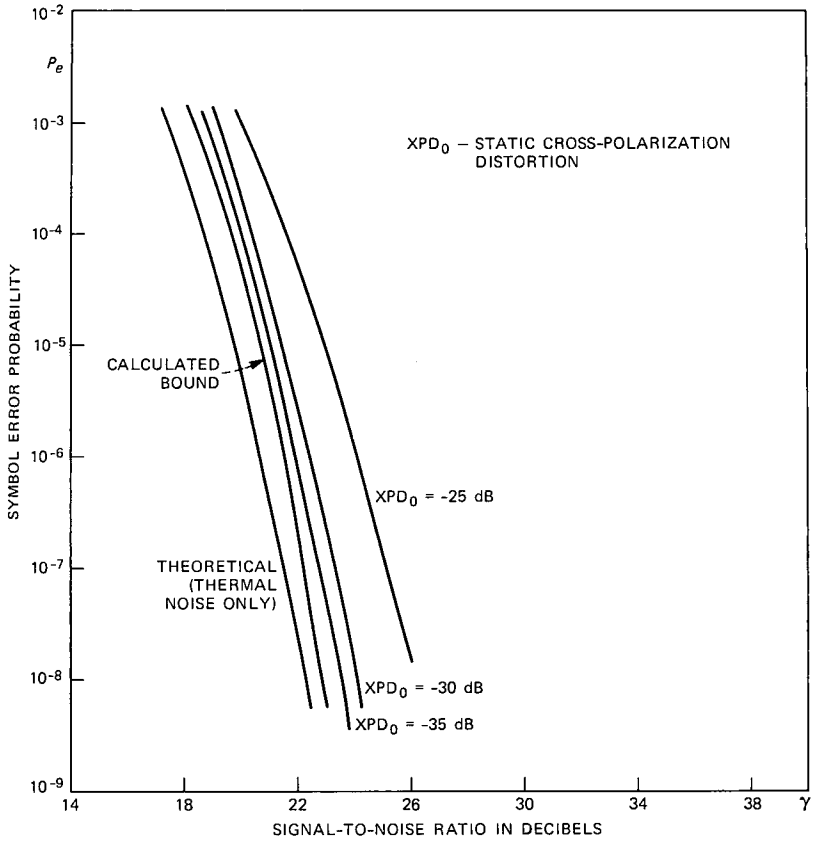

Fig. 3—Probability of error vs. s/n for dual 16 QAM without canceler; no fading exits.

and show the bounds in eqs. (18) and (23) in Fig. 5 for different XPD_0s. High values of XPD_0s could occur in poorly aligned antenna systems. As Fig. 5 illustrated, the LMS canceler and the diagonalizer behave quite differently. The LMS canceler improves the performance significantly even at rather poor XPDs, e.g., $XPD_0 = -5$ dB, while the diagonalizer is almost useless for such a case. As the XPD_0 value is improved, e.g., for a $XPD_0 = -25$ dB, the performance of the two cancelers becomes the same. This is because as XPD increases, the diagonalizer coefficients grow in a direction to cancel XPD, while neglecting the thermal noise completely; consequently, the noise power in each channel is increased strongly. The LMS canceler, however, by minimizing the combined noise and XPD power, produces an acceptable performance. On the other hand, as XPD is improved, the diagonalizer becomes as attractive as the LMS canceler since there is

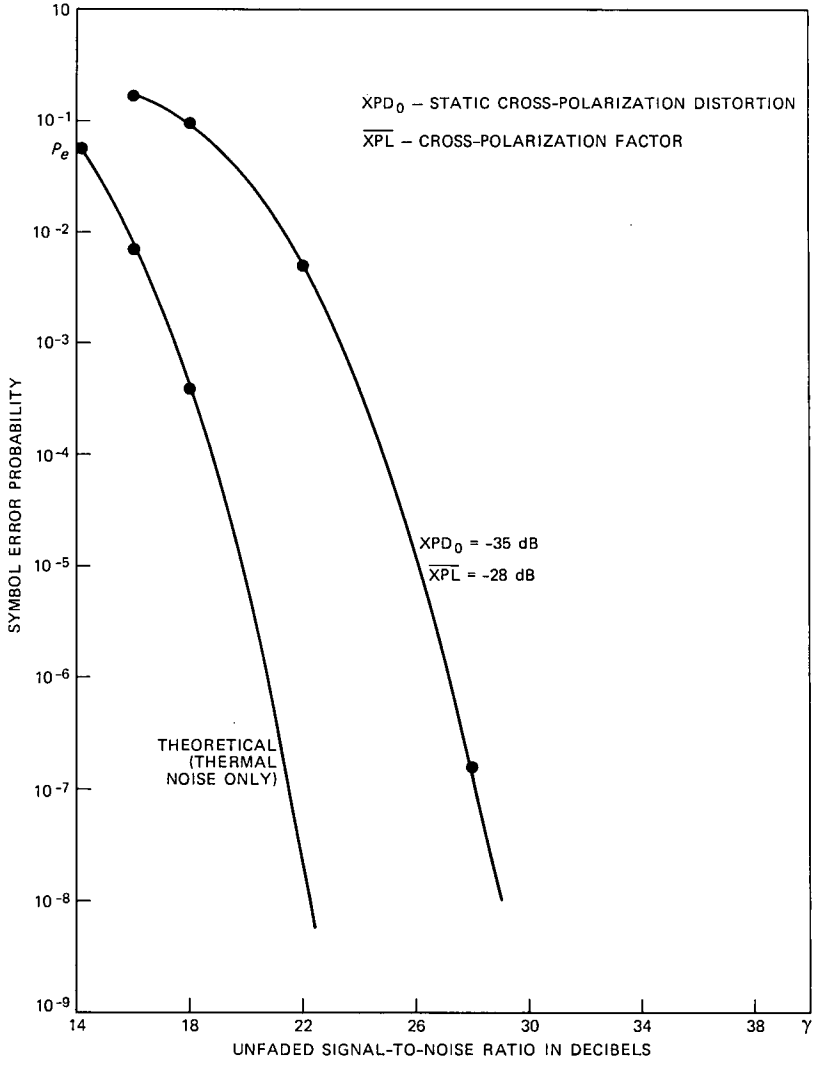

Fig. 4—Probability of error vs. s/n for dual 16 QAM without canceler; 5-dB flat fade applied.

not much XPD to cancel; consequently, there is not much noise enhancement. However, over fading channels where XPD, dB can even be positive, use of the LMS canceler will ensure a more reliable system.

We then apply 5-dB flat fade and draw the average error rate bounds for both cancelers as a function of fade level in Fig. 6. As we see, the XPD is removed for a practically reasonable static XPD. The horizon-

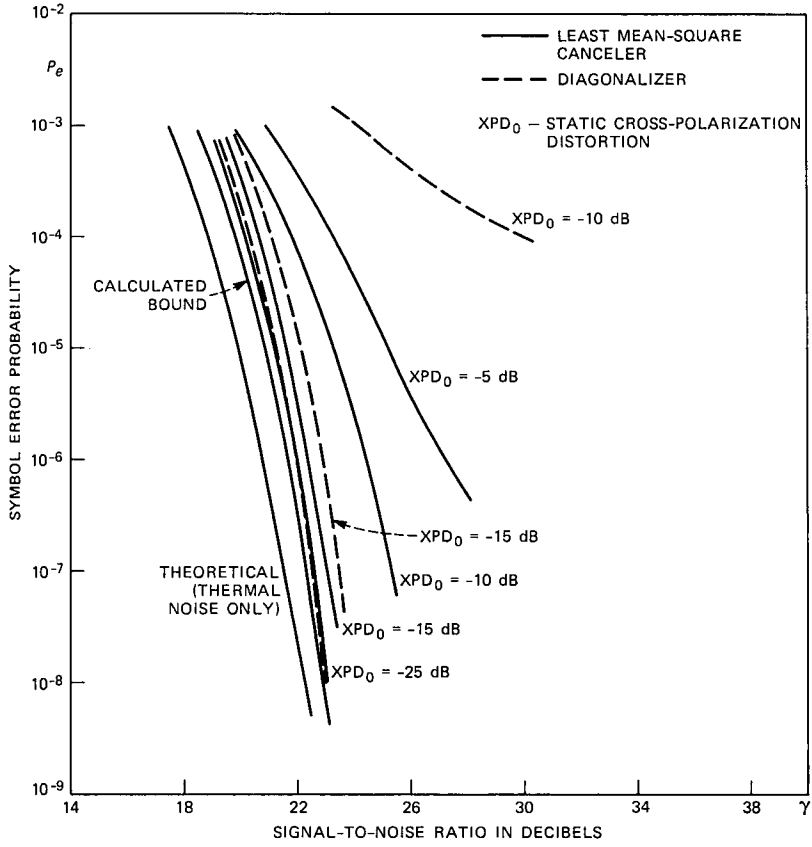

Fig. 5—Probability of error vs. s/n for dual 16 QAM with canceler; no fading exists.

tal translation of the curves reflects the 5-dB signal power loss due to fade since we have employed unfaded s/n in sketching these figures.

Note that rain fading increases the system noise temperature as follows. If we assume the noise temperature of the receiver and the following stages to be T_0, and in the presence of rain, T_p, the increased system noise temperature in rain is

$$T_p = T_0 + (1 - v)T_{\text{rain}},$$

where

$$v = |a_{ii}| = \text{in-line fade level}$$

$$T_{\text{rain}} = \text{effective temperature of the rain.}$$

For example, for a flat fade of 5 dB and rain temperature of 280K, the

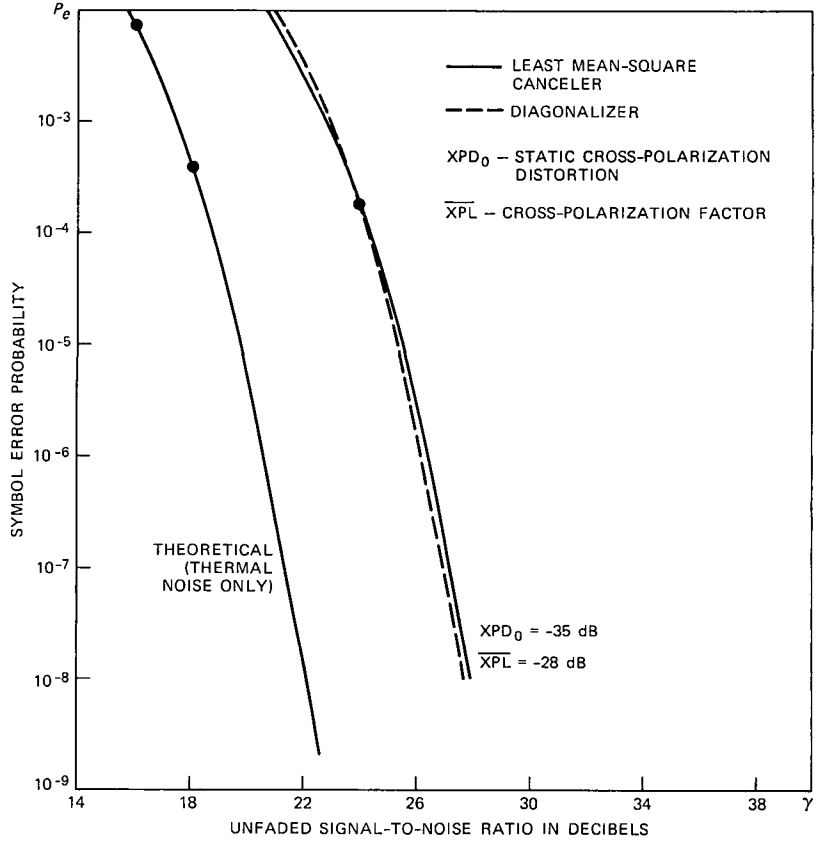

Fig. 6—Probability of error vs. s/n for dual 16 QAM with canceler; 5-dB flat fade applied.

system noise temperature increases by 122.5K. The additional increase in noise temperature will further translate the curves in Fig. 6 to the right, horizontally. In practice the noise power increase has to be factored in system power budget.

VI. CONCLUSIONS

In this paper we studied the performance of dual-polarized, M-ary QAM signals in terms of average probability of error as a function of s/n, x-pol distortion, and fade level. An x-pol cancellation method operating at baseband was suggested. Two different adaptation methods were considered in calculating the canceler coefficients. In particular, the performance was evaluated with and without the XPD cancellation for 16-QAM signals in dual polarization with or without fade. The results indicate that without applying some kind of x-pol

cancellation, dual polarization of M-ary QAM signals is not feasible. The results also indicate that the adaptive algorithm employed in cross-polarization interference cancellation should take into account noise power reduction.

REFERENCES

1. T. S. Chu, "Restoring the Orthogonality of Two Polarization in Radio Communication Systems, I," B.S.T.J, *50*, No. 9 (November 1971), pp. 3063–9.
2. T. S. Chu, "Restoring the Orthogonality of Two Polarization in Radio Communication Systems, II," B.S.T.J, *52*, No. 3 (March 1973), pp. 319–29.
3. M. L. Steinberger, "Design of a Terrestrial Cross Pol Canceler," IEEE ICC, Philadelphia, June 1982, pp. 2B.6.1–5.
4. A. F. Culmone, "Polarization Diversity with Adaptive Channel Decoupling," IEEE NTC, New Orleans, December 1975, pp. 25–22 to 25–27.
5. E. Nichols and J. Proakis, "Maximum Likelihood Detection of Digital Signals in the Presence of Interchannel-Interference," Int. Symp. on Inf. Theory, Sweden, January 1976.
6. T. S. Chu, "Microwave Depolarization of an Earth-Space Path," B.S.T.J, *59*, No. 6 (July 1980), pp. 987–1007.
7. A. Papoulis, *Probability, Random Variables, and Stochastic Processes*, New York: McGraw-Hill, 1965, Chapter 11.
8. B. Widrow, "Adaptive Filters," *Aspects of Network and System Theory*, New York: Holt, Rinehart & Winston, 1971, pp. 563–87.
9. N. Amitay, "Signal-to-Noise Ratio Statistics for Nondispersive Fading in Radio Channels with Cross-Polarization Interference Cancellation," IEEE Trans. Commun., *COM-27*, No. 2 (February 1979), pp. 498–502.
10. T. S. Chu, "Rain-Induced Cross-Polarization at Centimeter and Millimiter Wavelengths," B.S.T.J, *53*, No. 8 (October 1974), p. 1557.
11. J. M. Wozencraft and I. M. Jacobs, *Principles of Communication Engineering*, New York: Wiley, 1965, pp. 47–106.

APPENDIX A

Derivation of Error Bound for the Diagonalizer

Consider one of the dual-polarized channels, e.g., channel 1. Using the Chernoff bound for the in-phase rail of the M-ary QAM signal and eq. (15) in Section 4.1,

$$P_{e_1} = P_r\{|z_R| > c\} \leq \exp(-\lambda c)\left(E\left\{\exp\left[-\lambda\delta\xi^2\cos(\phi) + \lambda\beta\xi^2 \cdot \sin(\phi) + \frac{\lambda}{a_{11}}n_{1R} - \frac{\lambda\xi}{a_{11}}\left(n_{2R}\cos(\phi_1) - n_{2I}\sin(\phi_1)\right)\right]\right\}\right), \quad (27)$$

where

$$\phi = \phi_1 + \phi_2.$$

Since the terms in the argument of the inner exponential are inde-

pendent of each other, given that ϕ and ϕ_1 are known, we can average over independent variables first and then take the average of the result with respect to phase variables. So,

$$P_{e_1} \leq \exp(-\lambda c) E_{\phi,\phi_1}\Bigg\{E_\delta[\exp(-\lambda\delta\xi^2\cos\phi)]\cdot E_\beta[\exp(\lambda\beta\xi^2\sin\phi)] \cdot E_{n_{1R}}\left[\exp\left(\frac{\lambda}{a_{11}} n_{1R}\right)\right]\cdot E_{n_{2R}}\left[\exp\left(-\frac{\lambda\xi}{a_{11}} n_{2R}\cos(\phi_1)\right)\right] \cdot E_{n_{2I}}\left[\exp\left(\frac{\lambda\xi}{a_{11}} n_{2I}\sin(\phi_1)\right)\right]\Bigg\}, \tag{28}$$

where δ and β are the real and imaginary parts of a uniformly distributed, complex-valued random variable. We now calculate the statistical averages in eq. (28):

$$\Gamma_1 = E_{n_{1R}}\left[\exp\left(\frac{\lambda}{a_{11}} n_{1R}\right)\right] = \exp\left[\frac{\lambda^2}{2a_{11}^2}\sigma_n^2\right]$$

$$\Gamma_2 = E_\delta\{\exp(-\lambda\delta\xi^2\cos\phi)\} = \frac{2}{L}\sum_{i=1}^{L/2}\cosh\{\lambda\xi^2 c(2i-1)\cos(\phi)\}.$$

And, since

$$\frac{2}{L}\sum_{i=1}^{L/2}\cosh\{(2i-1)x\} \leq \exp\left[\frac{L^2-1}{3}\frac{x^2}{2}\right],$$

then,

$$\Gamma_2 \leq \exp\left[\frac{\lambda^2\xi^4c^2}{2}\frac{L^2-1}{3}\cos^2(\phi)\right].$$

Similarly,

$$\Gamma_3 = E_\beta\{\exp(\lambda\beta\xi^2\sin(\phi))\} \leq \exp\left[\frac{L^2-1}{3}\frac{\lambda^2\xi^4c^2}{2}\sin^2(\phi)\right]$$

$$\Gamma_4 = E_{n_{2R}}\left\{\exp\left(-\frac{\lambda\xi}{a_{11}} n_{2R}\cos(\phi_1)\right)\right\} = \exp\left[\frac{\lambda^2\xi^2\sigma_n^2}{2a_{11}^2}\cos^2(\phi_1)\right]$$

$$\Gamma_5 \leq E_{n_{2I}}\left\{\exp\left(\frac{\lambda\xi}{a_{11}} n_{2I}\sin(\phi_1)\right)\right\} \leq \exp\left[\frac{\lambda^2\xi^2\sigma_n^2}{2a_{11}^2}\sin^2(\phi_1)\right].$$

Therefore,

$$E_{\phi,\phi_1}\{\cdot\} = \exp\left[\frac{L^2-1}{3}\,\frac{\lambda^2\xi^4c^2}{2} + \frac{\lambda^2\sigma_n^2}{2a_{11}^2} + \frac{\lambda^2\xi^2\sigma_n^2}{2a_{11}^2}\right]$$

and

$$P_{e_1} \leqslant \exp\left[-\lambda c + \lambda^2\sigma_n^2\left(\frac{1}{2a_{11}^2} + \frac{L^2-1}{3}\,\frac{\xi^4c^2}{2\sigma_n^2} + \frac{\xi^2}{2a_{11}^2}\right)\right]. \tag{29}$$

If we repeat the derivation for $P_{e_2} = P_r\{|z_I| > c\}$, because of the symmetry, we will find out that the result is the same as for P_{e_1}; i.e.,

$$P_e = \frac{L-1}{2L}\,(P_{e_1} + P_{e_2}).$$

We now calculate the least upper bound on P_{e_1} by minimizing the argument of the exponential in eq. (29) with respect to λ. The result for

$$\lambda_{\min} = \frac{c}{\sigma_n^2\left[\dfrac{1}{a_{11}^2} + \dfrac{L^2-1}{3}\cdot\dfrac{\xi^4c^2}{\sigma_n^2} + \dfrac{\xi^2}{a_{11}^2}\right]}$$

is

$$P_e \leqslant \frac{(L-1)}{L}\exp\left\{-\frac{3}{2(L^2-1)}\,\frac{\gamma|a_{11}|^2}{1+\gamma\xi^4|a_{11}|^{2+}\xi^2}\right\}. \tag{30}$$

For channel 2 we find a similar result using $|a_{22}|^2$ in eq. (30) instead of $|a_{11}|^2$.

APPENDIX B

Derivation of Error Bound for the LMS Canceler

The derivation of error bound is somewhat tedious in this case. We employ the decision variables of eq. (22) of Section 4.1 and after some mathematical manipulations, find their real and imaginary parts. For example, for channel 1, by introducing

$$\nu = |a_{11}| \quad \text{and} \quad \phi = \phi_1 + \phi_2 \tag{31}$$

$$\hat{z}_{1R} = \mathrm{Re}\{\hat{\alpha}_1 - \tilde{\alpha}_1\} = \frac{1}{H}\,[A\cdot\delta_1 + B\cdot\delta_2 - C\cdot\beta_2 + D\cdot n_{1R} - E\cdot n_{1I} + F\cdot n_{2R} - G\cdot n_{2I}]$$

$$\hat{z}_{1I} = \mathrm{Im}\{\hat{\alpha}_1 - \tilde{\alpha}_1\} = \frac{1}{H}\,[A\cdot\beta_1 + B\cdot\beta_2 + C\cdot\delta_2 + D\cdot n_{1I} + E\cdot n_{1R} + F\cdot n_{2I} + G\cdot n_{2R}],$$

where

$$A = -(\nu^2\sigma_n^2 + \nu^2\xi^2\sigma_n^2 + \sigma_n^4)$$

$$B = \xi\nu^2\sigma_n^2[\cos\phi_1 + \cos\phi_2]$$

$$C = \xi\nu^2\sigma_n^2[\sin\phi_1 - \sin\phi_2]$$

$$D = \nu^3 + \nu\sigma_n^2 - \nu^3\xi^2\cos\phi$$

$$E = \nu^3\xi^2\sin\phi$$

$$F = -\nu^3\xi\cos\phi_1 + [\nu^3\xi^3 + \nu\xi\sigma_n^2]\cos\phi_2$$

$$G = -\nu^3\xi\sin\phi_1 - [\nu^3\xi^3 + \nu\xi\sigma_n^2]\sin\phi_2$$

$$H = [\nu^2\xi^2 + \nu^2 + \sigma_n^2]^2 - 2\nu^4\xi^2[1 + \cos\phi]. \tag{32}$$

In a similar manner as in Appendix A, we find an upper bound on $P_{e_1} = P_r\{|\hat{z}_{1R}| > c\}$ using the Chernoff bound.

Following the method used in Appendix A, we define

$$\Gamma_0 = E_{\delta_1}\left\{\exp\left(\lambda\left(\frac{A}{H}\right)\delta_1\right)\right\} = \frac{2}{L}\sum_{i=1}^{L/2}\cosh\left\{\lambda\left(\frac{A}{H}\right)(2i-1)c\right\}$$

$$\leqslant \exp\left[\frac{\lambda^2c^2}{2}\,\frac{L^2-1}{3}\left(\frac{A}{H}\right)^2\right].$$

Similarly,

$$\Gamma_1 \leqslant \exp\left[\frac{\lambda^2c^2}{2}\,\frac{L^2-1}{3}\left(\frac{B}{H}\right)^2\right]$$

and

$$\Gamma_2 \leqslant \exp\left[\frac{\lambda^2c^2}{2}\,\frac{L^2-1}{3}\left(\frac{C}{H}\right)^2\right].$$

Also,

$$\Gamma_3 = E_{n_{1R}}\left\{\exp\left(\lambda\left(\frac{D}{H}\right)n_{1R}\right)\right\} = \exp\left[\frac{\lambda^2}{2}\,\sigma_n^2\left(\frac{D}{H}\right)^2\right].$$

Similarly,

$$\Gamma_4 = \exp\left[\frac{\lambda^2}{2}\,\sigma_n^2\left(\frac{E}{H}\right)^2\right],$$

so

$$\Gamma_5 = \exp\left[\frac{\lambda^2}{2}\,\sigma_n^2\left(\frac{F}{H}\right)^2\right]$$

and

$$\Gamma_6 = \exp\left[\frac{\lambda^2}{2}\,\sigma_n^2\left(\frac{G}{H}\right)^2\right].$$

Therefore, using the Chernoff bound,

$$P_{e_1} \leqslant E_\Phi\left\{\exp\left[-\lambda c + \frac{\lambda^2 c^2}{2}\,\frac{L^2-1}{3}\,\frac{A^2+B^2+C^2}{H^2} + \frac{\lambda^2}{2}\,\sigma_n^2\,\frac{D^2+E^2+F^2+G^2}{H^2}\right]\right\},$$

where $E_\Phi\{\cdot\}$ is the expectation with respect to ϕ. We can minimize the argument of the $\exp\{\cdot\}$ with respect to λ. The least upper bound corresponds to

$$P_{e_1} \leqslant E_\Phi\left\{\exp\left[-\frac{3}{2(L^2-1)}\cdot\frac{\gamma\nabla(\phi)}{\gamma\Theta(\phi)+\Delta(\phi)}\right]\right\}. \tag{33}$$

This bound is conditioned on ϕ_1 and ϕ_2, so by taking the average over ϕ_1 and ϕ_2, the actual bound can be obtained. In eq. (33)

$$\begin{aligned}\Theta(\phi) &= A^2 + B^2 + C^2\\ \Delta(\phi) &= D^2 + E^2 + F^2 + G^2\\ \nabla(\phi) &= H^2.\end{aligned}$$

Hence,

$$\begin{cases}\Theta(\phi) = (\nu^2\sigma_n^2 + \nu^2\xi^2\sigma_n^2 + \sigma_n^4)^2 + 2\xi^2\nu^4\sigma_n^4(1+\cos\phi)\\ \Delta(\phi) = \nu^2(\nu^4 + \sigma_n^4 + 2\nu^2\sigma_n^2 + \nu^4\xi^4 + \nu^4\xi^2 + \nu^4\xi^6\\ \qquad\qquad + 2\nu^2\xi^4\sigma_n^2 + \xi^2\sigma_n^4) - 2\nu^4\xi^2[\nu^2\xi^2 + 2\sigma_n^2 + \nu^2]\cos\phi\\ \nabla(\phi) = \{(\nu^2 + \nu^2\xi^2 + \sigma_n^2)^2 - 2\nu^4\xi^2(1+\cos\phi)\}^2.\end{cases} \tag{34}$$

Since ϕ_1 and ϕ_2 are two independent random variables that are uniformly distributed over $(-\pi, \pi)$ and $\phi = \phi_1 + \phi_2$, the probability density function of ϕ is

$$f_\Phi(\phi) = \frac{1}{2\pi}\left(1 - \frac{1}{2\pi}\,|\phi|\right), \qquad 0 \leqslant |\phi| \leqslant 2\pi. \tag{35}$$

By using $f_\Phi(\phi)$, we can calculate the statistical average of the right-hand side of the bound in eq. (33) and find the least upper bound on P_{e_1}. Again, by symmetry

$$P_{e_2} = P_r\{|\hat{z}_{1I}| > c\} = P_{e_1},$$

so

$$P_e = \frac{L-1}{2L}\{P_{e_1} + P_{e_2}\} = \frac{L-1}{L} P_{e_1}$$

and

$$P_e \leqslant \frac{L-1}{L} \int_0^{2\pi} \frac{1}{\pi}\left(1 - \frac{\phi}{2\pi}\right) \cdot \exp\left\{-\frac{3}{2(L^2-1)} \cdot \frac{\gamma\nabla(\phi)}{\gamma\Theta(\phi) + \Delta(\phi)}\right\} d\phi, \quad (36)$$

in which $\gamma = \frac{L^2-1}{3}\frac{c^2}{\sigma_n^2}$ and $\nabla(\phi)$, $\Theta(\phi)$, and $\Delta(\phi)$ are defined in eq. (34).

APPENDIX C

Derivation of Error Bound for the Baseline System

If we use a similar approach,

$$P_e \leqslant \frac{L-1}{L} \exp(-\lambda c) \cdot E\left\{\exp\left\{\lambda\xi\delta_2\cos(\phi_1) - \lambda\xi\beta_2\sin(\phi_1) + \frac{\lambda}{|a_{11}|} n_{1R}\right\}\right\}. \quad (37)$$

Following what was done in Appendices A and B,

$$\Gamma_1 = E_{n_{1R}}\left[\exp\left\{\frac{\lambda n_{1R}}{|a_{11}|}\right\}\right] = \exp\left\{\frac{\lambda^2\sigma_n^2}{2|a_{11}|^2}\right\}$$

$$\Gamma_2 = E_{\delta_2}\left[\exp\left\{\lambda\xi\delta_2\cos(\phi_1)\right\}\right]$$

$$= \frac{2}{L}\sum_{j=1}^{L/2} \cosh[(2j-1)c\lambda\xi\cos(\phi_1)]$$

$$\leqslant \exp\left[\frac{\lambda^2\xi^2c^2}{2}\frac{L^2-1}{3}\cos^2(\phi_1)\right]$$

$$\Gamma_3 = E_{\beta_2}\left[\exp\left\{-\lambda\xi\beta_2\sin(\phi_1)\right\}\right]$$

$$= \frac{2}{L}\sum_{j=1}^{L/2} \cosh[(2j-1)c\lambda\xi\sin(\phi_1)]$$

$$\leqslant \exp\left[\frac{\lambda^2\xi^2c^2}{2}\frac{L^2-1}{3}\sin^2(\phi_1)\right]. \quad (38)$$

Therefore,

$$P_e \leq \frac{(L-1)}{L} \exp(-\lambda c) \cdot E_{\phi_1}\{\Gamma_1 \cdot \Gamma_2 \cdot \Gamma_3\}$$

or

$$P_e \leq \frac{(L-1)}{L} \exp\left[-\lambda c + \frac{1}{2} \frac{\lambda^2}{|a_{11}|^2} \sigma_n^2 + \frac{1}{2} \frac{L^2-1}{3} \lambda^2 c^2 \xi^2\right]. \quad (39)$$

By minimizing the argument of $\exp[\cdot]$ with respect to λ and substituting $\lambda_{\min}$ in eq. (37), the corresponding least upper bound is

$$P_e \leq \frac{(L-1)}{L} \exp\left[-\frac{3}{2(L^2-1)} \frac{\gamma |a_{11}|^2}{1+\gamma \xi^2 |a_{11}|^2}\right], \quad (40)$$

where

$$\gamma = \frac{L^2-1}{3} \frac{c^2}{\sigma_n^2},$$

and, similarly, the probability of error for channel 2 can be obtained by substituting $|a_{22}|^2$ instead of $|a_{11}|^2$ in eq. (40).

AUTHOR

Mohsen Kavehrad, B.S. (Electrical Engineering), 1973, Tehran Polytechnic Institute; M.S. (Electrical Engineering), 1975, Worcester Polytechnic Institute; Ph.D. (Electrical Engineering), 1977, Polytechnic Institute of New York; Fairchild Industries, 1977–1978; GTE, 1978–1981; AT&T Bell Laboratories, 1981—. At Fairchild Mr. Kavehrad worked on NASA space communications analysis projects. At GTE he worked in satellite communications and computer communication networks areas. At AT&T Bell Laboratories he is a member of the Radio Transmission Laboratory, where his current work involves exploratory studies in microwave radio subsystems. He teaches Communication Theory courses at the Northeastern University Continuing Education Program. He is a Technical Associate Editor for the IEEE Communications Magazine. Member, IEEE, Sigma Xi.